

# On-line Bandwidth Control for Quality of Service Mapping in Telecommunication Networks

Mario Marchese, *Senior Member, IEEE*, Maurizio Mongelli, *Student Member, IEEE*

**Abstract**—In telecommunication networks, a *Quality of Service* (QoS) mapping problem arises when different transport technologies (e.g., IP, ATM, MPLS, DVB) are employed to support the network services. The QoS mapping involves the change of encapsulation format, the need to aggregate traffic, as well as the channel degradation counteraction. In this work, a novel rate control mechanism is developed to face the mentioned problems. By exploiting *Infinitesimal Perturbation Analysis* to capture the network performance sensitivity, we obtain an adaptive control law, suited for on-line control on the basis of traffic samples acquired during the system evolution. Neither *certainty equivalent* assumptions are made on the stochastic environment, nor *closed-form* expressions of the chosen performance metric are required.

## I. INTRODUCTION

THE Internet traffic flows interconnecting users located in different sites of the world are routed throughout different proprietary networks, called *Autonomous Systems* (ASes), managed by different *Service Providers* (SPs). The Internet is composed of up to 10000 ASes and their number is rapidly growing. Each SP may choose a specific transport technology to offer QoS guarantees to users, e.g., *Internet Protocol* (IP), *Asynchronous Transfer Mode* (ATM), *Multiple Protocol Label Switching* (MPLS), *Digital Video Broadcasting* (DVB). Technology heterogeneity characterizes present and future Internet. It is true also for wireless portions of the overall network. Solutions to map QoS among different ASes and also among network portions implementing diverse QoS technologies need to be studied and applied.

In this perspective, the *Broadband Satellite Multimedia* (BSM) architecture, developed by the *European Telecommunications Standardization Institute* (ETSI), is a good example [1]. It separates the layers identified as *Satellite Dependent* (SD) and as *Satellite Independent* (SI). The interface between SI and SD layers is defined through SI-SAPs (*Satellite Independent – Service Access Points*), which are located in the gateways of satellite ASes.

The key point is that QoS requirements are defined at SI level, but they need to flow through the SI-SAPs and be implemented at SD layers. In this view, the paper envisages the QoS mapping among different ASes, by taking the SI-SAP interface as a reference. In other words, SI-SAP is the separation interface between two different technologies and, even if the problem is solved for ETSI SI-SAP, it may be

representative of a wider QoS mapping problem. A novel control scheme for the optimization of the bandwidth provision at the SD layer is proposed. The aim is to “map” the QoS defined at the SI layer into the SD technology, as if the satellite portions were transparent to the rest of the network.

The remainder of the paper is organized as follows. In the next section we detail the characteristics of the QoS mapping problem. Then, in section III, we formulate the related optimization problem. In section IV, some heuristics are summarized to tackle the envisaged problems and, in section V, we develop our optimized approach. Simulation results are proposed in section VI and conclusions and future work in Section VII.

## II. QoS MAPPING OVER BSM TECHNOLOGY

In general, interworking between networks implementing different technologies originates two main problems: **1)** the change of information unit (*encapsulation*) and **2)** the *need to aggregate* traffic. To help understand, we summarize in Fig. 1 the queue model describing the QoS mapping operations performed at the SI-SAP interface. ATM is chosen as SD transport technology together with the *ATM Adaptation Layer 5* (AAL5) encapsulation of IP packets.

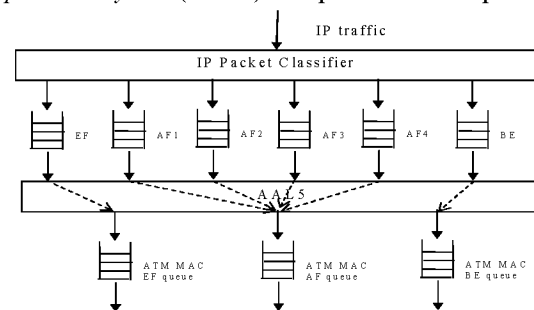


Fig. 1. SI-SAP interface [1]. SI layer (IP) over SD layer (ATM).

It is generally accepted in the BSM industry that at the IP level of the SI-SAP interface between 4 and 16 queues are manageable for different IP classes. On the other hand, for hardware implementation reasons, below the SI-SAP, these classes can further be “mapped” into the SD queues which can be from 2 to 4 [1]. In the case reported, 1 SD queue is dedicated to *Expedite Forwarding* (EF) traffic (e.g., mission critical data, voice), 1 for all the *Assured Forwarding* (AF) classes (e.g., real time data, stream video) and 1 for *Best Effort* (BE) (e.g., file transfer, web access).

Another reason for traffic aggregation relies in the limited capabilities of some transport technologies concerning

Authors are with the Department of Communication, Computer and Systems Science (DiST), University of Genoa, Via Opera Pia 13, 16145 Genoa, Italy (e-mail: {dama, mopa}@dist.unige.it).

traffic classification. An example may be represented by the IP *Differentiated Service* (DiffServ) methodology that uses a limited number of classes in IPv4. This leads to the creation of heterogeneous traffic flows (i.e., flows requiring diverse QoS guarantees) when different trunks (coming, for example, from ATM or MPLS network portions) must be aggregated together when conveyed through an IPv4 DiffServ core [2]. The same problem arises also in MPLS environments where the DiffServ traffic classification must be mapped into the limited MPLS queueing structure of network routers [3].

### III. PROBLEM FORMULATION

#### A. Fading counteraction

Another reason for concentrating our attention on the SI-SAP model is the need to emphasize a topical problem related to QoS mapping over wireless environments: degradation of the transmission channel due to fading. When a traffic flow (e.g., coming from a wired network) is conveyed to a wireless portion (e.g., a satellite or a terrestrial wireless core), due to the presence of variable channel degradation conditions, an additional bandwidth is required to maintain the desired QoS. We briefly summarize the mathematical model used to describe the fading counteraction in the paper. Let  $\theta^{SD}(t)$  be the service rate assigned to a traffic buffer at the SD layer at time  $t$ . The effect of fading can be modeled as a reduction of the bandwidth actually “seen” by the buffer. The reduction is represented by a variable  $\phi(t)$ . At time  $t$ , the “real” service rate  $\hat{\theta}^{SD}(t)$  (available for data transfer) is:

$$\hat{\theta}^{SD}(t) = \theta^{SD}(t) \cdot \phi(t); \quad \phi(t) \in [0, 1] \quad (1)$$

The reduction of the bandwidth may be due to the increase in the bandwidth required to maintain a fixed *Bit Error Rate* (BER) at the physical layer through *Forward Error Correction* (FEC) codes [4].

#### B. Stochastic fluid model and optimization problem

We are now able to formalize the QoS mapping problem studied in this work. The chosen mathematical framework is based on a *Stochastic Fluid Model* (SFM) [5] of the traffic buffers. We take a simplified Fig. 1 as reference. We consider the presence of  $N$  SI queues and a single SD queue. Let  $\alpha_i^{SI}(t)$  be the *inflow rate* process entering the  $i$ -th traffic buffer at the SI layer at time  $t$ ,  $i = 1, \dots, N$ . For the control model investigated in this work, IP *Packet Loss Probability* (PLP) is the target performance metric. According to it, we exploit the SFM *loss volume* of the  $i$ -th SI buffer whose service rate is  $\theta_i^{SI}(t)$ . We denote it by  ${}^iL_V^{SI}(\alpha_i^{SI}(t), \theta_i^{SI}(t))$ . Let  $\alpha^{SD}(t)$  be the *inflow rate* process of the buffer at the SD layer at time  $t$ . The  $\alpha^{SD}(t)$  process derives from the *outflow rate* processes of the SI buffers

( $\beta_i^{SI}(t)$ ,  $i = 1, \dots, N$ ) or directly from the  $\alpha_i^{SI}(t)$  processes, if no buffering is applied at the SI layer. In any case, a change in the encapsulation format is applied when  $\alpha^{SD}(t)$  is produced. We denote the loss volume of the  $i$ -th traffic class within the SD core by  ${}^iL_V^{SD}(\alpha^{SD}(t), \theta^{SD}(t) \cdot \phi(t))$ . It is a function of the following elements: SD inflow process  $\alpha^{SD}(t)$  (deriving from the aggregation of SI outflow processes and from the transport technology change), fading process  $\phi(t)$  and SD bandwidth allocation  $\theta^{SD}(t)$ . No analytical expressions for  ${}^iL_V^{SD}(\cdot)$  is available, since there are no instruments for the mathematical description of the statistical behaviour of the packets belonging to a specific connection within an aggregated trunk.

We suppose that resource allocation of SI can satisfy the required QoS at the SI level. Here, the key problem is to “equalize” the QoS measured at the SD layer in dependence of the QoS at the SI layer.

The optimization problem can now be stated. The **QoS Mapping Optimization** (QoSMO) **Problem** looks for the optimal bandwidth allocation  ${}^{Opt}\theta^{SD}(t)$ , so that the cost function  $J(\cdot, \theta^{SD}(t))$  is minimized:

$${}^{Opt}\theta^{SD}(t) = \arg \min_{\theta^{SD}(t)} J(\cdot, \theta^{SD}(t)); \quad J(\cdot, \theta^{SD}(t)) = E_{\omega \in \Theta} L_{NV}(\cdot, \theta^{SD}(t))$$

$$L_{NV}(\cdot, \theta^{SD}(t)) = \sum_{i=1}^N \left[ {}^iL_V^{SI}(\alpha_i^{SI}(t), \theta_i^{SI}(t)) - {}^iL_V^{SD}(\alpha^{SD}(t), \theta^{SD}(t) \cdot \phi(t)) \right]^2 \quad (2)$$

We denote a *sample path* of the system by  $\omega$ , i.e., a realization of the stochastic processes involved in the problem ( $\phi(t)$ ,  $\alpha_i^{SI}(t)$ ,  $i = 1, \dots, N$ ) according to the statistical behaviour of the traffic sources and to the channel degradation and with  $E_{\omega \in \Theta}(\cdot)$  the mean over the set  $\Theta$  of all the possible sample paths. All the variables are considered at the time instant  $t$  to stress the fact that we are looking for an adaptive control law, able to counteract non-stationary conditions (e.g., where the number of sources in each traffic class or the fading level change over time).

We must note that even if a closed-form formula for the cost function  $J(\cdot, \theta^{SD}(t))$  were available, it would require a-priori assumptions on the traffic sources. Since our aim is to avoid any *certainty equivalent* assumption, we investigate a way to spread the solution of (2) over time, by exploiting a *sensitivity estimation* procedure “capturing” the current bandwidth need of the SD buffer.

### IV. HEURISTIC APPROACHES

Traditionally, the QoS mapping is heuristically performed by the SP. We now summarize two possible operative proposals, alternative to the optimization framework proposed here.

1) The first one is dedicated to IP over ATM, it is much used in industry and acts as follows. The increase in

bandwidth necessary for SD layer can be foreseen by means of the so-called *CellTax* effect due to the change of encapsulation format (e.g., when applying AAL5 encapsulation to produce an ATM-based frame). Since, during the generation of the SD frame, two octets (for the AAL5 overhead) need to be added to each IP packet, the number of SD cells for each IP packet is:

$$\# \text{ATMCells} = \left\lceil \frac{\text{DimIPPacket} + 2}{48} \right\rceil \quad (3)$$

where *DimIPPacket* denotes the IP packet's size in bytes and 48 is the payload of an ATM cell in bytes. Hence, it is possible to compute the overall overhead due to the encapsulation format of the SD frame and the percentage bandwidth increase in the SD core, denoted in the following with *CellTax*:

$$\text{CellTax} = \frac{\# \text{ATMCells} \cdot 53 - \text{DimIPPacket}}{\text{DimIPPacket}} \quad (4)$$

where 53 is the overall size of an ATM cell in bytes. Then, a possible forecast for the SD bandwidth allocation (called **CellTaxAllocation** heuristic) is ruled by the heuristic allocation law (5) each time the SI rate provision  $\theta^{\text{SI}}$  changes.

$$\theta^{\text{SD}} = \text{CellTax} \cdot \theta^{\text{SD}} = (1 + \text{CellTax}) \cdot \theta^{\text{SI}} \quad (5)$$

A similar heuristic can be employed when the transport technologies of interest are different, e.g., in case of a QoS mapping involving IPv6 over IPv4 or IPv4 over MPLS or DVB. As we will show in the experimental part of the paper, *CellTax* allocation underestimates the necessary SD rate provision. A deeper insight into the statistical behaviour of the flows is necessary.

2) The second approach is based on the concept of *equivalent bandwidth* [6], which is defined as the “*minimum rate allocation necessary to maintain a specific level of QoS to a given flow*”. For the QoS problem investigated here, traditional equivalent bandwidth techniques are hardly applicable. In general, they are based on the statistical characterization of the traffic generated by the users' applications. Sophisticated mathematical descriptions are proposed to this aim, based on proper traffic descriptors (*peak rate, mean rate, maximum burst size, etc.*) [6]. Unfortunately, being the inflow process  $\alpha^{\text{SD}}$  the result of the outflow processes of the SI buffers, the aforementioned user oriented traffic descriptors can be applied with big difficulty. The only equivalent bandwidth technique, immediately applicable in this context, has been introduced in [6] and is ruled by (6) below. Being:  $k = 1, 2, \dots$  the time instants of the SD rate reallocations,  $m_{\alpha^{\text{SD}}}(k)$  and  $\sigma_{\alpha^{\text{SD}}}(k)$  the *mean* and the *standard deviation*, respectively, of the SD inflow process measured over the time interval  $[k, k+1]$ ; the SD bandwidth provision  $\theta^{\text{SD}}(k+1)$ , assigned for time interval  $[k+1, k+2]$ , may be computed as a function of the measured statistics  $m_{\alpha^{\text{SD}}}$  and  $\sigma_{\alpha^{\text{SD}}}$  through:

$$\theta^{\text{SD}}(k+1) = m_{\alpha^{\text{SD}}}(k) + a(\varepsilon) \cdot \sigma_{\alpha^{\text{SD}}}(k) \quad (6)$$

$a(\varepsilon) = \sqrt{-2 \ln(\varepsilon) - \ln(2\pi)}$ ;  $\varepsilon$  represents the upper bound on the allowed PLP. It must be chosen as the most stringent PLP required at the SI layer. This allows guaranteeing all SI PLP thresholds in the SD trunk, but it may introduce bandwidth waste [2]. This approach is identified as **Equivalent Bandwidth approach** (EqB).

## V. THE OPTIMIZED APPROACH

In this section, we detail our optimized approach.

To exploit the solution of (2), we capture the temporal behaviour of each single performance level  ${}^i L_V^{\text{SD}}(\cdot)$  through on-line measurements and perform the SD rate reallocations accordingly to them. To reach the aim, we exploit the cost function  $L_{\Delta V}(\cdot)$  derivative that can be obtained from (7) as:

$$\frac{\partial L_{\Delta V}(\cdot; \theta^{\text{SD}})}{\partial \theta^{\text{SD}}} = 2 \cdot \sum_{i=1}^N \frac{\partial {}^i L_V^{\text{SD}}(\theta^{\text{SD}})}{\partial \theta^{\text{SD}}} [{}^i L_V^{\text{SD}}(\theta^{\text{SD}}) - {}^i L_V^{\text{SI}}(\theta^{\text{SI}})] \quad (7)$$

Due to the application of *Infinitesimal Perturbation Analysis* (IPA) [5], each  $\frac{\partial {}^i L_V^{\text{SD}}(\theta^{\text{SD}})}{\partial \theta^{\text{SD}}}$  component can be obtained in real time on the basis of some traffic samples, acquired during the system evolution. Let  $[k, k+1]$  be the time interval between two consecutive SD reallocations  $\theta^{\text{SD}}(k)$  and  $\theta^{\text{SD}}(k+1)$  (we call it a *decision epoch*). The periods of time in which the buffer is not empty are defined as *busy periods*. The derivative estimation is computed at the end of the  $k$ -th decision epoch as:

$$\left. \frac{\partial {}^i L_V^{\text{SD}}(\theta^{\text{SD}})}{\partial \theta^{\text{SD}}} \right|_{\hat{\theta}^{\text{SD}}(k)} = \phi(k) \cdot \sum_{\zeta=1}^{N_k^i} \left. \frac{\partial {}^i L_{k,\zeta}^{\text{SD}}(\theta^{\text{SD}})}{\partial (\theta^{\text{SD}})} \right|_{\hat{\theta}^{\text{SD}}(k)} \quad (8)$$

$$\left. \frac{\partial {}^i L_{k,\zeta}^{\text{SD}}(\theta^{\text{SD}})}{\partial (\theta^{\text{SD}})} \right|_{\hat{\theta}^{\text{SD}}(k)} = -({}^i v_{\zeta}^k (\hat{\theta}^{\text{SD}}(k)) - {}^i \xi_{\zeta}^k (\hat{\theta}^{\text{SD}}(k))) \quad (9)$$

where  ${}^i L_{k,\zeta}^{\text{SD}}(\theta^{\text{SD}})$  is the  $\zeta$ -th contribution to the SD loss volume of  $i$ -th traffic class of each busy period  $B_k^{\zeta}$  within the decision epoch  $[k, k+1]$ ,  $\xi_{\zeta}^k$  is the start point of  $B_k^{\zeta}$ ,  $v_{\zeta}^k$  is the instant of time when the last loss occurs during  $B_k^{\zeta}$  and  $N_k^i$  is the number of busy periods within  $[k, k+1]$  for service class  $i$ . The key idea is to measure the contribution of the IP packets belonging to the  $i$ -th traffic class to the lengths of the busy periods of the SD buffer. These measures allow capturing the QoS received by the  $i$ -th traffic class within the aggregated trunk. The IPA-based derivative estimator (7) is then used to optimally tune the SD rate provision. The proposed optimization algorithm is based on the gradient method, whose descent step is ruled by (10) below. We denote by  $\eta_k$  the gradient stepsize and with  $k$  the reallocation time instant. The algorithm is called

**Reference Chaser Bandwidth Controller (RCBC).** It tracks the optimal solution  $^{Opt}\theta^{SD}(t)$  of the QoSMO problem (2) over time through the on-line gradient descent:

$$\theta^{SD}(k+1) = \theta^{SD}(k) - \eta_k \cdot \left. \frac{\partial L_{\Delta V}(\cdot; \theta^{SD})}{\partial \theta^{SD}} \right|_{\hat{\theta}^{SD}(k)} ; k = 0, 1, \dots \quad (10)$$

The employed gradient-based algorithm is a standard *stochastic approximation* [7] scheme, driven by the IPA-based derivative estimator (7).

Fig. 2 summarizes the role of the SI loss volume over the SD core in order to highlight the optimal operation point of the system, where the QoS thresholds (i.e., the SI and SD loss volumes) are equalized. For the sake of simplicity, a single SI traffic class is considered.

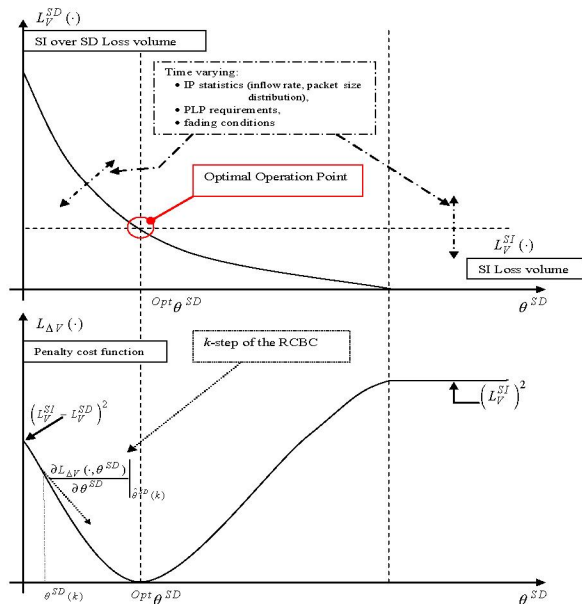


Fig. 2. Cost function and optimal operation point of the system.

Since both  $L_V^{SI}(\cdot)$  and  $L_V^{SD}(\cdot)$  are the loss volumes of traffic queues, they can be reasonably assumed to be continuous, differentiable, with a negative derivative in the service rate. As a consequence, the penalty cost function  $L_{\Delta V}(\cdot)$  is also continuous, differentiable with a unique minimum  $^{Opt}\theta^{SD}$ , as depicted in Fig. 2. The challenge is to automatically adapt  $^{Opt}\theta^{SD}$  to counteract time varying system conditions, namely, either when the required  $L_V^{SI}(\cdot)$  is redefined, or the traffic statistics and the fading change, thus varying the slopes of both  $L_V^{SI}(\cdot)$  and  $L_V^{SD}(\cdot)$ . Due to the regularity of the penalty cost function  $L_{\Delta V}(\cdot)$  in (2), the aforementioned gradient-based algorithm should track the  $^{Opt}\theta^{SD}$  value efficiently. The major concern is related to the stationarity of the involved stochastic processes. It is necessary to assume that the RCBC convergence toward a new operation point is faster than the changes of the stochastic environment. We will show in the simulation results the RCBC response in the presence of time varying

system conditions. The key point is to properly dimension both the gradient step size and the initial point of the gradient descent in (10).

## VI. SIMULATION RESULTS

In this section, we validate our rate control mechanism through simulations. An ad-hoc C++ simulator has been developed for the SI-SAP environment depicted in Fig. 1. The loss volumes actually measured at SI layer ( $L_V^{SI}(\cdot)$ ,  $i=1, \dots, N$ ) is chased by RCBC for all the results shown in the following.

### A. Encapsulation change

One IP queue and one ATM queue are taken into account for now and only the encapsulation problem is analyzed. We consider the case of a *Voice over IP (VoIP)* traffic, guaranteed at the SI layer, and carried along the ATM SD layer. Each VoIP source is modeled as an exponentially modulated on-off process, with mean on and off times (as for the ITU P.59 recommendation) equal to 1.008 s and 1.587 s, respectively. All VoIP connections are modeled as 16.0 kbps flows voice over RTP/UDP/IP. The IP packet size is 80 bytes. The required performance objective of a VoIP flow is less than 2% of PLP. We suppose that SI bandwidth  $\theta^{SI}$  has been already dimensioned in order to guarantee the required PLP constraint.

We compare the *CellTaxAllocation* strategy with our RCBC with the same size of IP and ATM buffers (fixed at 20 VoIP packets corresponding to 31 ATM cells) and by progressively increasing, from 70 to 110, the number of VoIP sources in the flow. The step is of 10 sources to stress the working conditions. The time interval between each change in the traffic flow is fixed to 3000 s. Similar results can be obtained by imposing a mean interarrival time of connection requests (this was validated by simulation results not reported here). To help the convergence, the *CellTax* heuristic (5) is used to initialize the gradient descent of RCBC. Each time the number of VoIP source changes (every 3000 seconds), the SD bandwidth allocation of RCBC is initialized through (5), and, every 30 s, a new SD bandwidth allocation  $\theta^{SD}(k)$  is performed through (10). Particular attention is necessary for the gradient stepsize to avoid strong bandwidth oscillations or a low convergence. We verified through simulation inspection that the convergence speed is maximized if the gradient stepsize is

tuned as  $\eta_k = \left. \frac{\partial L_{\Delta V}(\cdot; \theta^{SD})}{\partial \theta^{SD}} \right|_{\hat{\theta}^{SD}(k)} \cdot 6 \cdot 10^{-7}$ . Note that

$\eta_k \xrightarrow{k \rightarrow +\infty} 0$  since  $\theta^{SD}(k)$ ,  $k = 0, 1, \dots$  are driven by (10).

Fig. 3 shows the performance of *CellTaxAllocation*, which is not always able to guarantee the required PLP. On the other hand, the RCBC performance (reported in Fig. 4) is very satisfying. The two allocation techniques are compared with respect to the bandwidth provision in Fig. 5. The

*CellTaxAllocation* underestimates the required SD rate provision to correctly carry the VoIP flows.

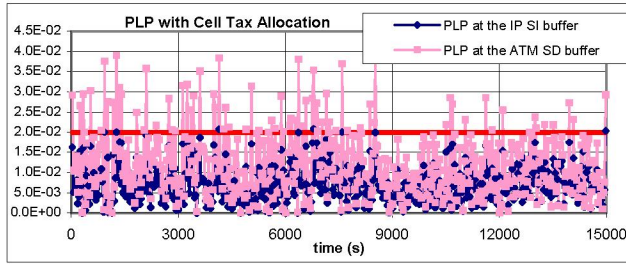


Fig. 3. Encapsulation change. PLP with CellTaxAllocation.

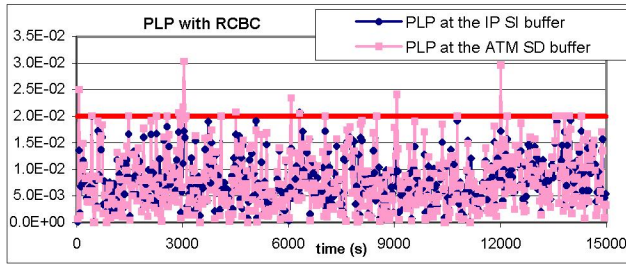


Fig. 4. Encapsulation change. PLP with RCBC.

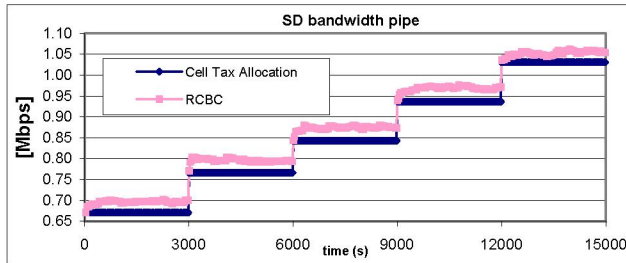


Fig. 5. Encapsulation change. SD allocation.

### B. Aggregation

We consider now the case of two SI traffic buffers. The first one offers a VoIP service to a flow composed of 30 sources with 64 kbps of peak rate. The SI service rate for VoIP ( $\theta_{VoIP}^{SI} = 232$  kbps, found through simulation inspection) assures a PLP less than  $10^{-2}$  (the SI buffer size for VoIP is 30 VoIP packets). The second one guarantees a video service whose PLP target is  $10^{-3}$ . Both the outputs of the SI buffers are conveyed towards a single queue at the SD layer. A DVB encapsulation (header 4 bytes, payload 184 bytes) (again through AAL5) of IP packets is implemented in this case. The SD buffer size is 300 DVB cells.

Fig. 6 depicts the increase (with respect to the SI layer) of the bandwidth provision at the SD layer necessary to guarantee the required PLP targets. Different values of SD buffer size and video traces are used. Video data are taken from [8]. They are H.263 encoded and have an average bit rate of 260 kbps as well as a peak bit rate ranging from 1.3 to 1.5 Mbps, depending on the specific trace. The SI rate allocation for video ( $\theta_{Video}^{SI}$ ) ranges from 310 to 370 kbps.

The increase is computed as  $\frac{Opt \theta^{SD} - (\theta_{VoIP}^{SI} + \theta_{Video}^{SI})}{\theta_{VoIP}^{SI} + \theta_{Video}^{SI}}$ . The

$Opt \theta^{SD}$  is obtained through RCBC and guarantees the maintenance of the PLP required by VoIP and video services within the DVB tunnel. Fig. 6 outlines that, from the operative viewpoint, in the aggregation case presented, the *Service Provider* (responsible for the satellite core performance) must increase the bandwidth provision related to the traffic entering the SD core up to 50% in order to assure the same QoS offered on the SI portions.

RCBC and EqB are compared in Figs. 7-9 where the video PLP over the DVB trunk, the average and the variance of SD allocations over the entire simulation horizon (about 3 hours) are shown with respect to the “Jurassic Park I” video trace (for the other traces similar comments may be applied). RCBC performs the reallocations every 7 minutes. We denote by  $T$  the time interval between two consecutive SD rate reallocations when EqB is applied. We employ different values of  $T$  for EqB.

Using RCBC, the averaged PLPs obtained in the SD trunk for VoIP, not shown here, and video are  $1.23 \cdot 10^{-4}$  and  $1.04 \cdot 10^{-3}$ , respectively. It is clear from Figs. 7-9 that RCBC finds the optimal operation point of the system, namely, the minimum SD bandwidth provision needed to track the measured SI QoS thresholds. On the other hand, when EqB allocates more bandwidth than necessary, the SD PLP for video is much lower than  $10^{-3}$  and viceversa when the SD allocation is underestimated. This is due to the noise introduced by the on-line estimation of the EqB traffic parameters ( $m_{\alpha^{SD}}$  and  $\sigma_{\alpha^{SD}}$ ), thus leading to strong SD rate oscillations, in particular for  $T = 7, 3.5$  and  $2.33$  minutes (see Fig. 9). The high variance of EqB with  $T = 7$  explains why EqB obtains a larger PLP when it adopts the same decision epoch dimension of RCBC (see the 2<sup>nd</sup> and the 3<sup>rd</sup> column from the left of Fig. 7), even if it allocates a larger service rate on average (see the first two columns from the left of Fig. 8).

### C. Fading countermeasure

The object of performance evaluation is now the fading phenomenon. An aggregate trunk of 50 VoIP on-off sources constitutes the traffic process at the SI-SAP interface. ATM is used as SD layer. Only one IP queue and one ATM queue are isolated for this test. The simulation time is 133.0 minutes. The target PLP is below 2%. The buffer size is set to 1600 bytes (20 VoIP packets) for the SI layer and to 70 ATM cells for the SD layer. The RCBC decision epoch lasts 1 minute. The employed fading process comes from reference [4]. The gradient descent is initialized through the *CellTax* heuristic every time a change of fading is detected (this information derives from the physical layer). As is shown in Fig. 10, the fading process determines strong peaks of channel degradation, especially in the time interval [4800, 6000]. The PLP measured at the SD layer is depicted in Fig. 11. The required PLP (graphically reported in Fig. 11 as a red line) is guaranteed almost all the time. Only 4 peaks of performance degradation appear when the worst fading

levels take place, corresponding to 5 minutes of performance decrease (around  $5 \cdot 10^{-2}$  instead of  $2 \cdot 10^{-2}$ ) within the entire simulation period. RCBC effectively produces a quick response to channel variations and is able to maintain the desired QoS. The bandwidth allocations of both SD and SI layers (the former including the additional rate to match fading counteraction) are finally shown in Fig. 12.

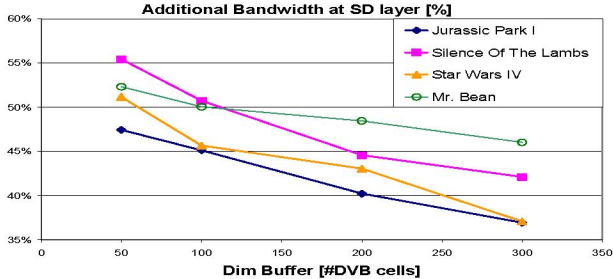


Fig. 6. Aggregation. Bandwidth increase at the SD layer using RCBC.

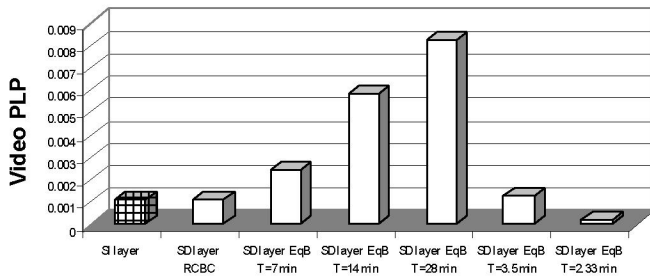


Fig. 7. Aggregation. Video PLP. "Jurassic Park I" trace.

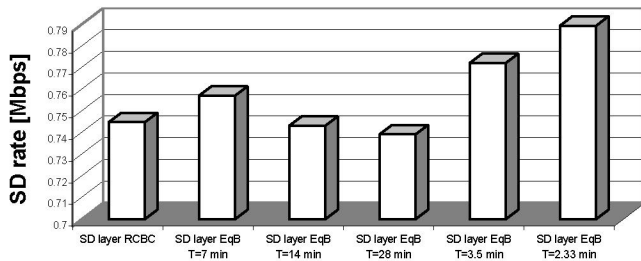


Fig. 8. Aggregation. Average SD rate. "Jurassic Park I" trace.

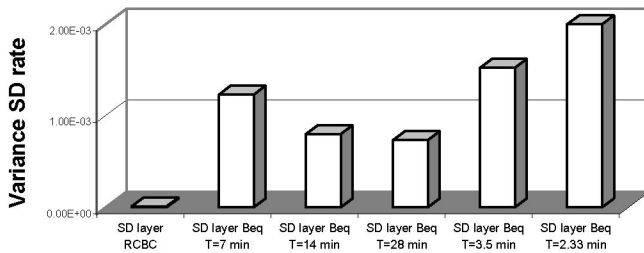


Fig. 9. Aggregation. Variance SD rate. "Jurassic Park I" trace.

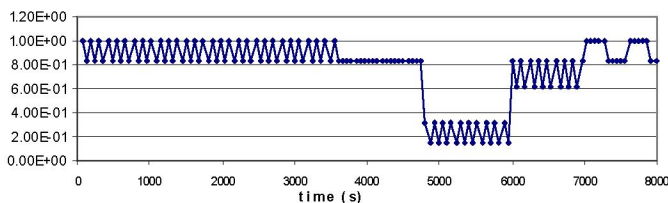


Fig. 10. Fading. Bandwidth reduction factor  $\phi(t)$  (from [4]).

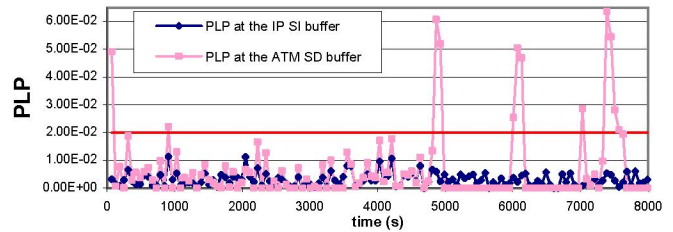


Fig. 11. Fading. PLP at the SI and SD layers using RCBC.

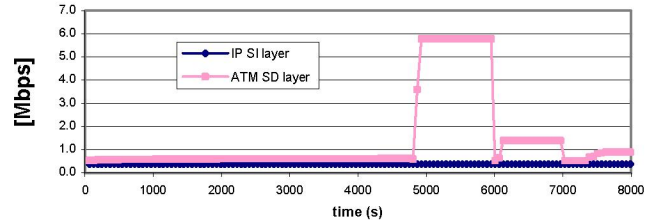


Fig. 12. Fading. RCBC allocations.

## VII. CONCLUSION AND FUTURE WORK

A novel bandwidth allocation technique has been proposed in order to manage the QoS mapping problem arising when different transport technologies are used to support the QoS. It is able to react to time varying system conditions, always guaranteeing the minimal allocation necessary for the maintenance of the QoS.

Future work may concern the application of the proposed methodology for other interworking architectures. End-to-end performance control is currently under investigation, too. It is also worth noting that the *delay* and *delay jitter* metrics can be managed in a similar way by exploiting the *buffer workload* sensitivity derived in [5].

## REFERENCES

- [1] ETSI. Broadband Satellite Multimedia. Services and Architectures, BSM Traffic Classes. Technical Specification, TS 102 295 V1.1.1, Feb. 2004.
- [2] E. Fortunato, M. Marchese, M. Mongelli, A. Raviola, "QoS Guarantee in Telecommunication Networks: Technologies and Solutions," *Internat. J. of Commun. Sys.*, vol. 17, no. 10, Dec. 2004, pp. 935-962.
- [3] V. Fineberg, "QoS Support in MPLS Networks," MPLS/Frame Relay Alliance White Paper, May 2003 (<http://www.mfaforum.org>).
- [4] N. Celandroni, F. Davoli, E. Ferro, "Static and Dynamic Resource Allocation in a Multiservice Satellite Network with Fading," *Internat. J. of Satellite Commun. and Networking*, vol. 21, no. 4-5, July-Oct. 2003, pp. 469-487.
- [5] C. G. Cassandras, G. Sun, C. G. Panayiotou, Y. Wardi, "Perturbation Analysis and Control of Two-Class Stochastic Fluid Models for Communication Networks," *IEEE Trans. Automat. Contr.*, vol. 48, no. 5, May 2003, pp. 23-32.
- [6] R. Guérin, H. Ahmadi, M. Naghshineh, "Equivalent capacity and its application to bandwidth allocation in high-speed networks," *IEEE J. Select. Areas Commun.*, vol. 9, July 1991, pp. 968-981.
- [7] H. J. Kushner, G. G. Yin, *Stochastic Approximation Algorithms and Applications*, Springer-Verlag, New York, NY, 1997.
- [8] <http://www-tnk.ee.tu-berlin.de/research/trace/trace.html>.